Effects of Fusion Zone Size and Failure Mode on Peak Load and Energy Absorption of Advanced High-Strength Steel Spot Welds

DP800 and TRIP800 steels were studied under various welding parameters to determine the critical fusion zone size for nugget pullout

BY X. SUN, E. V. STEPHENS, AND M. A. KHALEEL

ABSTRACT. This paper examines the effects of fusion zone size on failure modes, static strength, and energy absorption of resistance spot welds (RSW) of advanced high-strength steels (AHSS). DP800 and TRIP800 spot welds were considered. The main failure modes for spot welds are nugget pullout and interfacial fracture. Partial interfacial fracture is also observed. The critical fusion zone sizes to ensure nugget pullout failure mode are developed for both DP800 and TRIP800 using limit load based analytical model and microhardness measurements of the weld cross sections. Static weld strength tests using cross-tension samples were performed on the joint populations with controlled fusion zone sizes. The resulting peak load and energy absorption levels associated with each failure mode were studied for all the weld populations using statistical data analysis tools. The results in this study show that AHSS spot welds with fusion zone size of $4\sqrt{t}$ cannot produce nugget pullout mode for both the DP800 and TRIP800 materials examined. The critical fusion zone size for nugget pullout shall be derived for individual materials based on different base metal properties as well as different heat-affected zone (HAZ) and weld properties resulting from different welding parameters.

Introduction

Because of their excellent strength and formability combinations, advanced high-strength steels (AHSS) offer the potential for improvement in vehicle crash performance without extra weight increase. Currently, two types of advanced high-strength steels are being used in the automotive industry. One is the dual-phase (DP) steel in which ferrite and martensite are the primary phases, and its mechanical properties are controlled by the martensite volume fraction and the ferrite grain size (Refs. 1, 2). The other kind is the transformation-induced plasticity (TRIP) steel, in which bainite and/or martensite, plus fine islands of retained austenite, are embedded in a fine-grained ferrite microstructure. The presence of retained austenite in TRIP steels enhances ductility at a particular strength level by means of phase transformation from austenite to martensite. This phenomenon involves formation of strain-induced martensite by deformation of metastable austenite and leads to the increase of strength, ductility, and toughness of the steel.

Dual-phase and TRIP steels are alloyed to control the amount and transformation of intercritically formed austenite. The carbon contents in these steels typically range from 0.05 to 0.2 wt-% C, and the manganese content may be up to 1.5 wt-%. In TRIP steels, Si or Al additions are also made to limit cementite formation, thus enhancing the amount of retained austenite present after isothermal transformation, and P may be added as a ferrite solid-solution strengthener (Ref. 1). Because of the relatively high carbon equivalents in AHSS, it should be anticipated that the steel microstructures in the heat-affected zone will be significantly modified by different welding processes.

Spot welds are the primary method of joining automotive structural components. A vehicle's structural performance depends in part on the welded-joint structural integrity (Refs. 3–5). It is well known that in some vehicle safety regulated systems, such as the fuel system, joint performance can dramatically alter the system performance. As a means of quality control for spot welds of mild steel, the domestic automotive industry has historically used destructive tests such as the peel test or chisel test to determine whether a satisfactory weld has been produced. The common criterion is that the average weld button diameter should be equal to or larger than $4\sqrt{t}$ (t defined as material thickness in mm). Undersized welds have an average weld button diameter larger than $2\sqrt{t}$ but less than $4\sqrt{t}$.

Defective welds have average weld button diameters less than or equal to $2\sqrt{t}$. Some welds that fail in the interfacial fracture mode in conventional steels would be considered unacceptable and would be rejected by the quality control inspector (Refs. 6, 7). Welding engineers have also adopted $4\sqrt{t}$ as the target button size for mild steels.

This historical criterion works well for spot welds of mild steel because the weld nugget has a significantly higher hardness (hence, yield strength) than the base material; therefore, nugget pullout around the heat-affected zone (HAZ) should be the desired failure mode based on fundamental mechanics strength estimation. Any mild steel weld joint that separates in the interfacial fracture mode would indicate incomplete fusion or small fusion zone size, and therefore, would not meet

KEYWORDS

AHSS
Automotive
Dual Phase
Heat-Affected Zone
Nugget
Resistance Spot Weld
TRIP

X. SUN, E. V. STEPHENS, and M. A. KHALEEL are with Pacific Northwest National Laboratory, Richland, Wash.

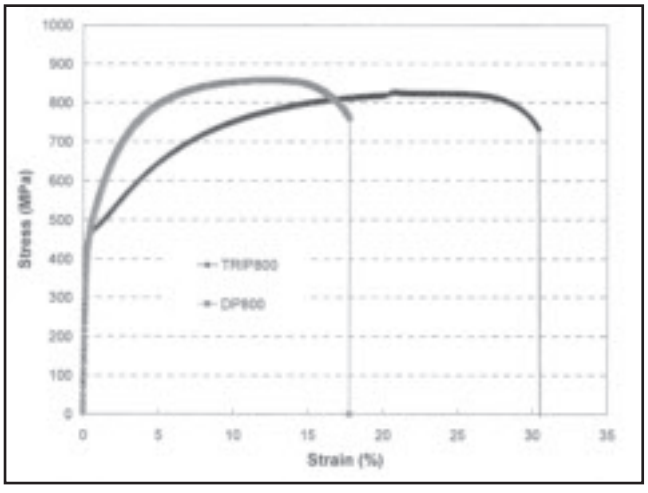

Fig. 1 — Comparison of base metal vs. strain curves.

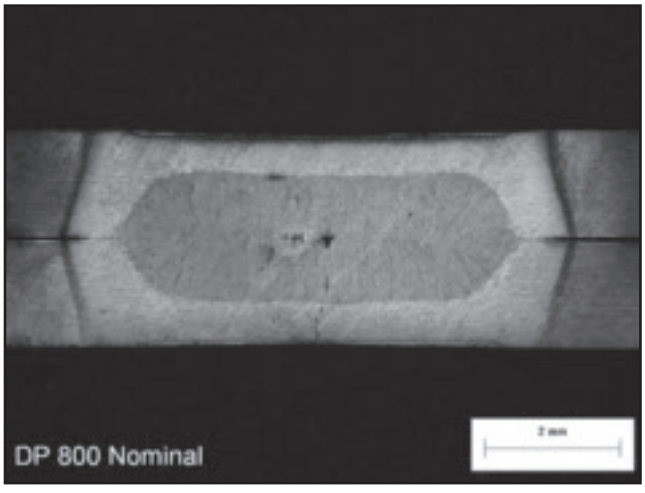

Fig. 2 — Metallurgical cross section for DP800 nominal weld.

the necessary joint strength requirements. The effectiveness of this criterion for evaluating AHSS spot weld, however, has not been adequately addressed in the automotive welding community; it was simply adopted from the mild steel practice and applied to AHSS spot welds.

In this paper, we examine the effects of fusion zone size on failure modes, static strength, and energy absorption of resistance spot welds of DP800 and TRIP800 under cross-tension loading condition.

The objectives of this study are 1) examine whether conventional weld size guidance of $4\sqrt{t}$ can produce nugget pullout failure modes for both DP800 and TRIP800 spot welds, 2) establish the influence of weld fusion zone size on failure mode for DP800 and TRIP800 spot welds, and 3) establish the effects of weld failure modes on its peak load and energy absorption levels for DP800 and TRIP800 welds.

The critical fusion zone sizes to ensure nugget pullout failure mode are developed for both DP800 and TRIP800 welds using the limit load based analytical model and the microhardness measurements of the weld cross sections (Refs. 6, 8). The critical weld fusion zone size for nugget pullout depends on the base metal mechanical properties as well as the properties of the weld zone and heat-affected zone. Static strength tests using cross-tension samples were performed on the joint populations with controlled fusion zone sizes. The peak load and energy absorption levels associated with each failure mode were then studied using statistical data analysis tools. The weld test results show that the weld fusion zone size is a critical factor in its static cross-tension performance in terms of failure mode, peak load, and energy absorption. The cross-tension test results also serve as validations for the critical fusion zone sizes developed. A similar approach has been used in studying the effects of fusion zone size and failure modes on the peak load and energy absorption levels of aluminum spot welds (Refs. 6, 8).

RSW Sample Preparation and Microhardness Comparison

The experimental work in this investigation consists of quasi-static tests of cross-tension welded samples of DP800 and TRIP800. DP800 sheet is 1.6 mm thick with galvanized coating, and TRIP800 sheet is 1.5 mm thick uncoated. Following the naming conventions for advanced high-strength steels, these two steel materials should have a minimum ultimate tensile strength (UTS) of 800 MPa. Room temperature stress vs. strain curves for the two materials are shown in Fig. 1, illustrating that both materials satisfy the minimum UTS requirement. TRIP800 exhibits much higher ductility by means of transformation-induced plasticity.

The RSW specimens were fabricated by Edison Welding Institute. Three weld sizes were achieved for each material: small, nominal, and large. The target fusion zone sizes for the small weld populations, i.e., 4.9 mm, are calculated based on the minimum button size criterion of $4\sqrt{t}$. The target fusion zone sizes for the nominal welds are based on the analytical estimations presented in the following section. The target fusion zone sizes for the large welds for both DP800 and TRIP800 were determined such that they are 1.4 mm larger than the corresponding nominal fusion zone sizes. The welding parameters used in the coupon fabrication process are summarized for all the sample populations in Table 1. The large populations were produced at expulsion levels

Table 1 — Welding Parameters Used for Coupon Fabrication

Material	1.6 mm DP800			1.5 mm TRIP800		
Weld population	Small	Nominal	Large	Small	Nominal	Large
Electrode	30-deg truncated cone electrodes with 7.9-mm face diameter			30-deg truncated cone electrodes with 7.9-mm face diameter		
Electrode force (lbf)	1150			1150		
Welding current (kA)	10.2	11	11.6	8.3	10.3	11.9
Weld time (cycle)	11	11	11	11	11	11
Hold time (cycle)	5	5	5	5	5	5
Target fusion zone size (mm)	4.9	5.6	7.0	4.9	6.4	7.8
Actual average fusion zone size (mm)	5.3	5.9	8.3	4.9	7.7	9.0

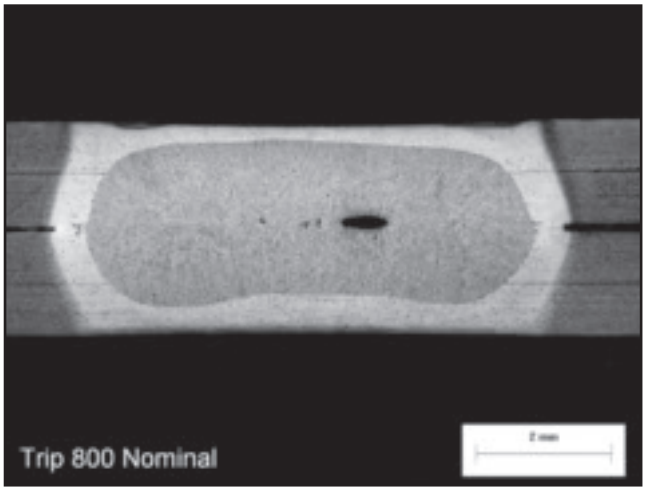

Fig. 3 — Metallurgical cross section for TRIP800 nominal weld.

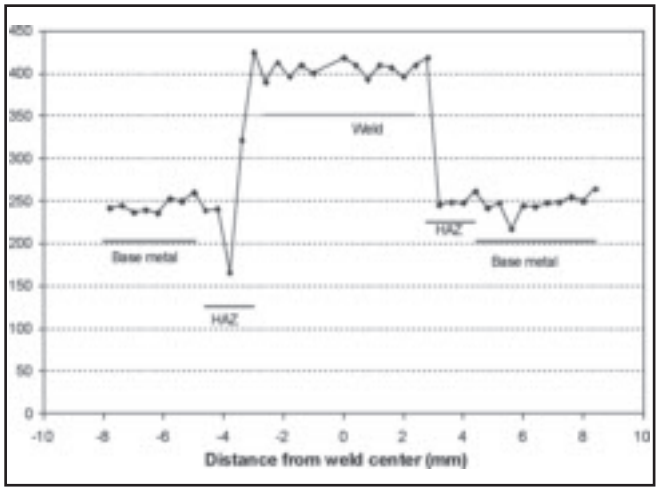

Fig. 4 — Microhardness measurement for the DP800 nominal weld.

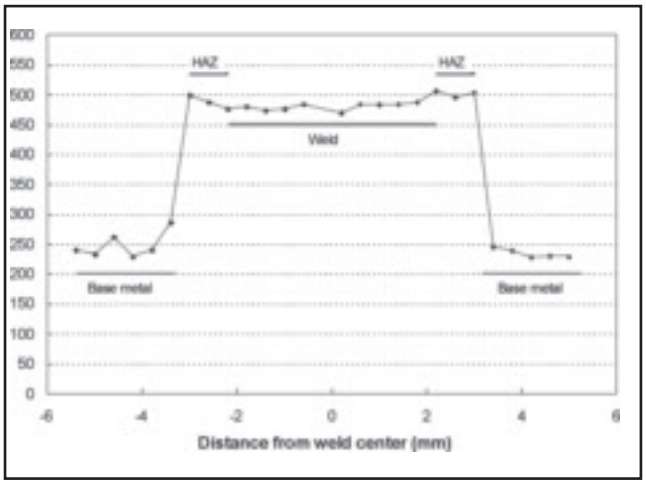

Fig. 5 — Microhardness measurement for the TRIP800 nominal weld.

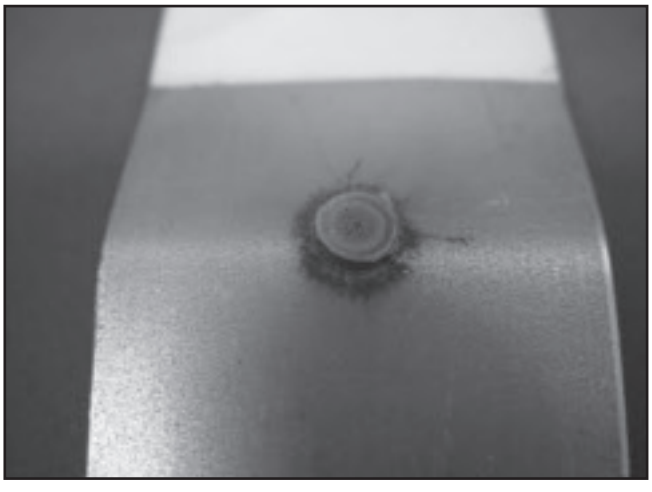

Fig. 6 — Pullout failure for DP800 spot welds.

using the electrodes listed in Table 1. Special fixtures were used to ensure the location of the welds to be in the width center of the specimens. Peel tests and metallographic cross sections were used to maintain the desired nugget diameters for all specimens.

Figures 2 and 3 show the typical weld metallurgical cross sections for DP800 and TRIP800 nominal populations, respectively. The micrographs in Figs. 2 and 3 indicate that TRIP800 has a much narrower heat-affected zone (HAZ) than the DP800 welds using the welding parameters listed in Table 1. This comparison also holds true for the welds in the small and large populations. It should be mentioned that the effects of Zn coating on nugget development have been taken into consideration in the welding parameters development, and that the welding parameters listed in Table 1 were developed specifically for these two materials and the corresponding target fusion zone sizes.

Standard metallographic preparation procedures were used to produce the weld cross sections. It should be noted that some degree of weld porosity exists on the weld centerline away from the weld periphery. The influence of weld porosities at different locations are discussed in the following sections.

Figures 4 and 5 depict the microhardness traverse for the nominal DP800 and the nominal TRIP800 welds. Base metal hardness levels for the two materials are about the same, roughly around 250 HV. Under the welding parameters listed in Table 1, TRIP800 weld has a harder fusion zone than the DP800 weld. The weld hardness profiles for both steel grades show an increase in HAZ hardness near the fusion boundary. For the DP800 welds, Fig. 4 also indicates a noticeable drop in HAZ hardness away from the fusion zone boundary. This phenomenon has been referred to as HAZ softening by other researchers (Refs. 9, 10). The softening is caused by increased martensite tempering through the HAZ approaching the weld. The degrees of softening depend on material chemistry, thermal mechanical processing as well as welding heat input (Ref. 10). In contrast, the HAZ away from the fusion zone for TRIP800 remains to be slightly harder than the weld metal. As is shown in the next section, the differences in the HAZ hardness, therefore yield strength levels, will dictate the differences in failure modes and the critical fusion zone sizes for the two materials, both with 800 MPa ultimate tensile strength level.

Analytical Failure Mode Prediction for AHSS Spot Welds under Cross-Tension Loading Condition

In this section, the limit-load-based approach is used similar to that described in

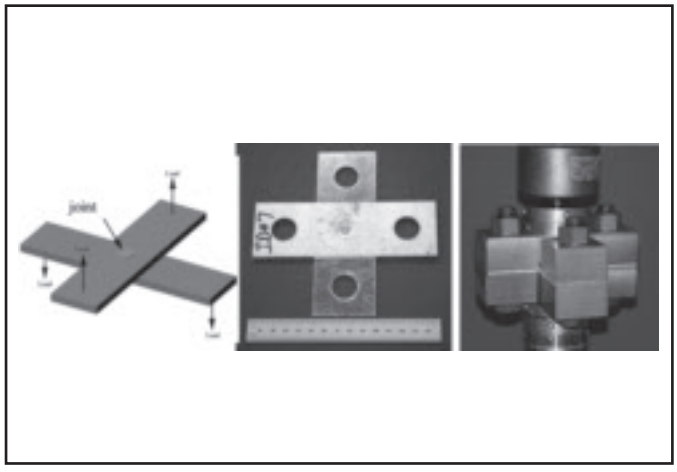

Fig. 7 — Cross-tension coupon design and test fixture.

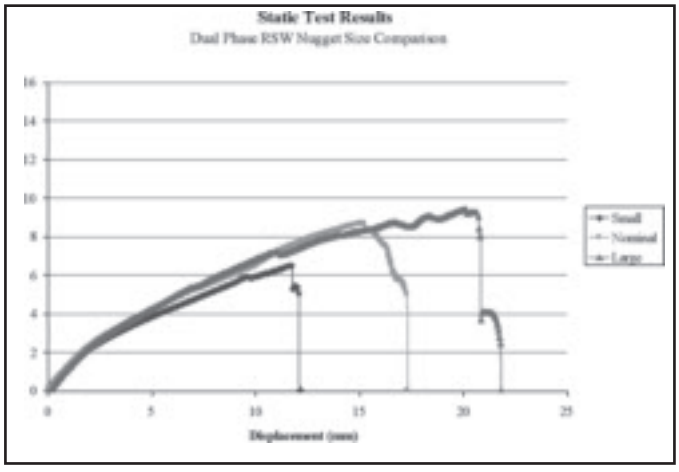

Fig. 8 — Typical load vs. displacement curves for DP800 welds.

Ref. 6 to predict joint failure mode and the associated critical fusion zone size for DP800 and TRIP800 spot welds under static cross-tension loading. As shown in Figs. 2–5, a typical cross section of an AHSS weld consists of base metal, fusion zone, and the region between the base metal and the fusion zone: the heat-affected zone. Again, the differences in the HAZ hardness for DP800 and TRIP800 would dictate that the two materials need different critical fusion zone sizes for nugget pullout under cross-tension loading.

Denote the weld fusion zone diameter as D and the sheet thickness as t. Assuming that the local weld region experiences near-axisymmetric deformation under cross-tension loading, the peak load for a weld to fail in interfacial fracture mode can be approximated as (Ref. 6)

$$F_{IF} = A_{total} \cdot \sigma_{y-weld} = \pi \cdot \frac{D^2}{4} \cdot \sigma_{y-weld} \quad (1)$$

where $\sigma_{y\text{-}weld}$ represents the tensile yield strength of the weld metal. The tensile yield strength of the weld metal is used instead of ultimate strength because this is a limit load analysis in which no local material hardening or necking is considered.

On the other hand, if the spot welds fail in button pullout mode, experiments have shown that failure normally occurs by through-thickness pullout in the heat-affected zone (Ref. 11). Therefore, the peak load for a weld to fail in nugget pullout mode under cross tension can be approximated as

$$F_{PO} = \pi \cdot D_{button} \cdot t \cdot \sigma_{y-HAZ} \quad (2)$$

In Equation 2, $\sigma_{y\text{-}HAZ}$ represents the yield strength of the heat-affected zone and D_{button} represents the diameter of the pullout button.

For welds with relatively narrow HAZ and no HAZ softening, fusion zone diameter D and button diameter D_{button} should be roughly the same since pullout failure occurs in the HAZ near the fusion zone root. However, for welds with wide HAZ ($\geq$ 1 mm) and HAZ softening, as in the current DP800 case, pullout failure often occurs at the transition region between the HAZ and the base metal — Fig. 6. Since the HAZ width is around 1 mm at each side of the fusion zone tip based on the results shown in Fig. 2, button diameter D_{button} can be estimated as (D+2) for the DP800 welds under examination.

Also note that $\sigma_{y\text{-}HAZ}$ is used instead of $\sigma_{y\text{-}HAZ\text{-}shear}$ as in the aluminum RSW case in Ref. 6. This is due to the fact that steel sheets used in resistance spot welding are relatively thin such that a significant amount of base metal rotation usually occurs around the weld nugget before final weld failure. The nuggets are actually pulled out from the base metal as opposed to being sheared out in the aluminum RSW. Similar treatment is also given for base metal rotation in Refs. 12 and 13. It should be mentioned that Equation 2 also assumes no significant weld indentation. If noticeable weld indentation occurs from the welding process, a reduced level of t should be used based on the actual residual sheet thickness around the weld periphery.

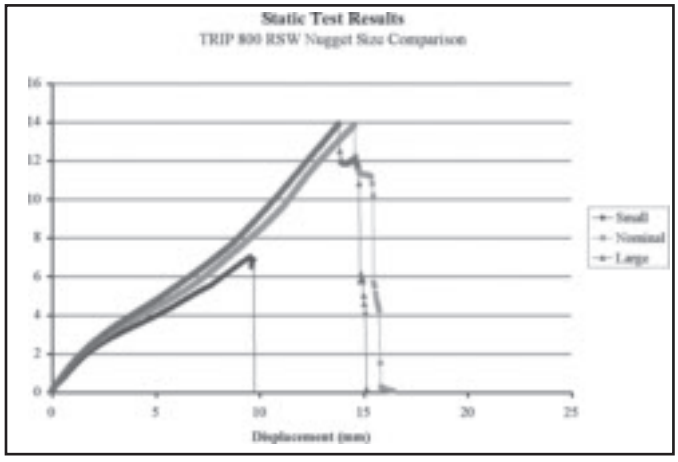

Fig. 9 — Typical load vs. displacement curves for TRIP800 welds.

The failure mode of a specific weld under cross-tension loading condition can then be determined by selecting the failure mode associated with the lower peak load level according to Equations 1 and 2 given the values of $\sigma_{y\text{-}weld}$ and $\sigma_{y\text{-}HAZ}$. In order to ensure pullout failure for a spot weld, the following inequality needs to be satisfied:

$$F_{PO} < F_{IF} \quad (3)$$

Relating material's tensile yield strength linearly with its microhardness value by a common coefficient C (Ref. 14), the critical fusion zone sizes for nugget pullout for DP800 and TRIP800 welds can be estimated by plugging in the hardness values in Figs. 4 and 5 into Equations 1–3

$$D800: \pi \cdot \left(D_{crit}^{DP800} + 2\right) \cdot t \cdot C \cdot 250 = \pi \cdot \frac{\left(D_{crit}^{DP800}\right)^2}{4} \cdot C \cdot 400 \Rightarrow \quad D_{crit}^{DP800} \cong 5.6(mm)$$

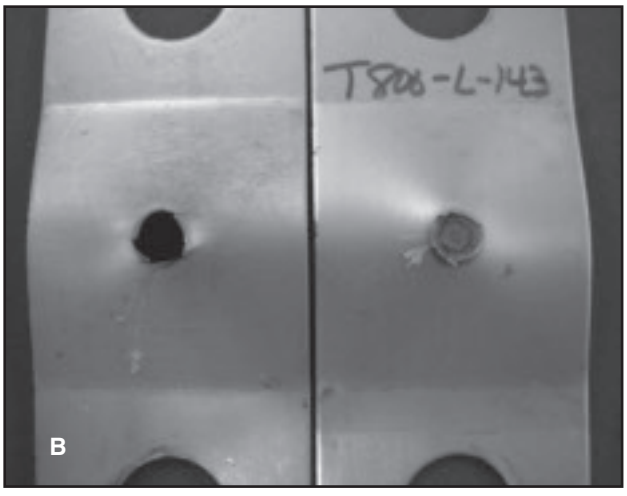

Fig. 10 — Different failure modes. A — Interfacial fracture; B — nugget pullout; C — partial interfacial fracture.

$$TRIP800: \pi \cdot D_{crit}^{TRIP800} \cdot t \cdot C \cdot 510 = \pi \cdot \frac{\left(D_{crit}^{TRIP800}\right)^2}{4} \cdot C \cdot 475 \Rightarrow \quad D_{crit}^{TRIP800} \cong 6.4(mm)$$

These critical values are used as the target fusion zone sizes for the nominal weld populations. Note that the predicted critical fusion zone sizes for nugget pullout for both DP800 and TRIP800 are larger than the conventional criteria of $4\sqrt{t}$ for mild steel. Also note that parameter C is cancelled out since it is on both sides of the above equations. Therefore, the absolute values of C are not critical in our formulation assuming the linear relationship between hardness and yield strength in the range studied. In the next section, experimetally measured weld performance data are used to illustrate the effects of different fusion zone sizes and different failure modes on weld performance.

Experimental Weld Strength Characterization

The cross-tension specimens and test fixture designs are shown in Fig. 7 for weld strength characterization. Quasi-static tests at a rate of 10 mm/min were performed on these specimens to determine their load vs. displacement curves. Figures 8 and 9 show the typical load vs. displacement curves for DP800 and TRIP800 welds. Thirty static tests were performed for each joint population in DP800. For TRIP800, 15 tests were performed for the small and large populations, and 30 tests were performed for the nominal population. It is interesting to note that even though welds in TRIP800 populations offer higher peak load than their respective DP800 counterparts, their energy absorption levels are about the same due to the reduced ductility level (displacement to failure) of the TRIP800 welds.

Both nugget pullout and interfacial fracture modes were observed for the cross-tension samples of DP800 and TRIP800 welds — Fig. 10A, B. In addition, partial interfacial fracture is also observed in which an irregular, smaller than fusion zone size button is produced — Fig. 10C. A detailed data analysis using statistical tools is presented in the next section to study whether different failure modes have a significant influence on the peak failure loads for these two populations.

Test Data Analysis

In this section, the test data were analyzed using two parameter Weibull distributions to study the influences of fusion zone size and failure mode on weld's peak load and energy absorption (Refs. 6, 8, and 15). The test results also serve as a good validation of the critical fusion zone predictions discussed in the previous section.

Assuming the available data points in each subpopulation of different failure modes are sufficient for statistical significance, the characteristics of the Weibull plots for interfacial fracture and nugget pullout modes can provide the median value as well as the degree of scatter for each failure mode (Ref. 15). Note that all the welds failed in partial interfacial fracture (Fig. 10C) are categorized as interfacial fracture during data processing such that only two major failure modes are analyzed for each weld population. This is also done because porosities such as those shown in Figs. 2 and 3 could potentially change the weld failure mode from interfacial fracture to partial interfacial fracture. In plotting results for different populations, empty symbols represent test cases failed in interfacial fracture and solid symbols represent test cases failed in nugget pullout mode.

DP800 Welds

Figure 11 shows the weld fusion zone distribution and the associated failure modes for the small, nominal, and large DP800 weld populations. It is interesting to note that both the small and the large weld populations have very tightly controlled weld sizes except for the three smallest welds in each population at the tail end of the distributions. However, these weld size abnormities do not have a great influence on the tail end shapes of

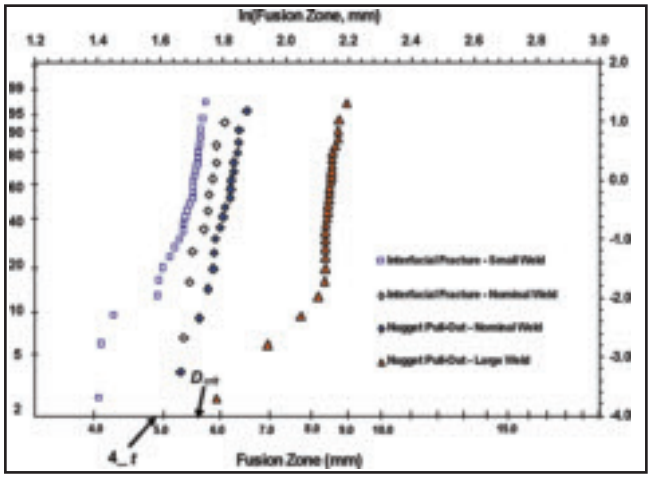

Fig. 11 — Fusion zone distribution and its effect on failure mode for DP800.

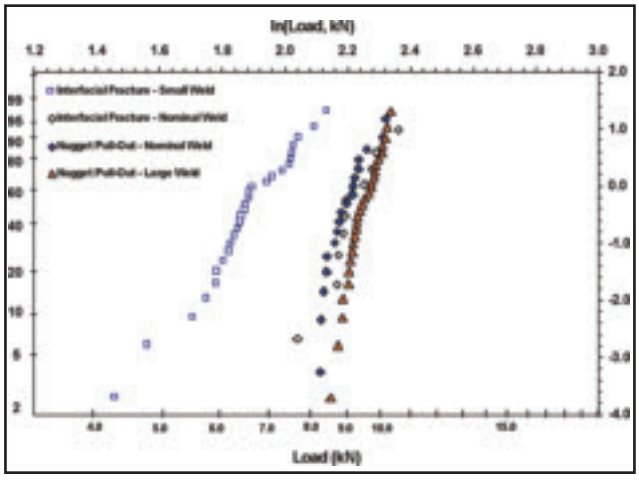

Fig. 12 — Peak lode distributions for three weld populations in DP800.

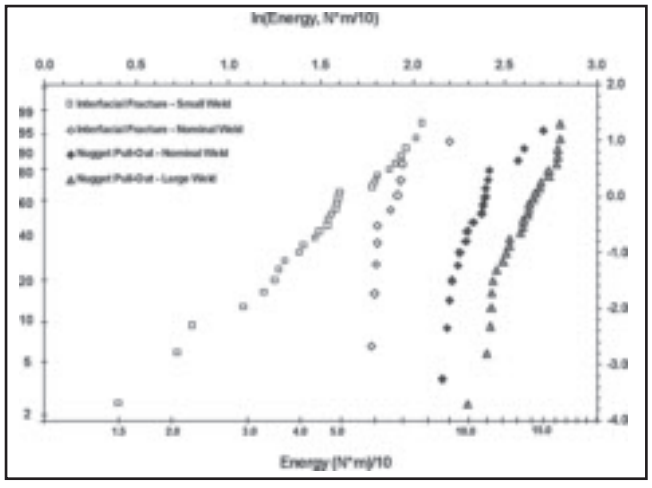

Fig. 13 — Distributions of energy absorption level for three weld populations in DP800.

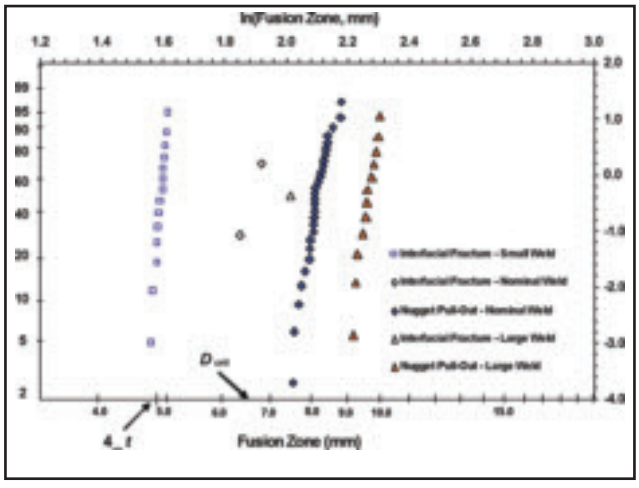

Fig. 14 — Fusion zone size distribution and its effect on failure mode for TRIP800.

the peak load and energy absorption distributions — Figs. 12, 13.

All the welds in the small population failed in interfacial fracture mode and all the welds in the large population failed in nugget pullout mode. Ten out of the 30 welds in the nominal population failed in interfacial fracture and the rest failed in nugget pullout. The occurrence of both failure modes within the nominal population validates our critical fusion zone size prediction. In addition, Fig. 11 indicates that the nominal welds failed in interfacial fracture do have smaller average fusion zone size than the nominal welds failed in nugget pullout. Figures 12 and 13 illustrate that even though different failure modes in the nominal population do not significantly influence the average peak-load distributions, nominal welds failed in pullout mode do provide much higher energy-absorption levels than the nominal welds failed in interfacial fracture. Results in Figs. 11–13 also indicate that at the conventionally recommended fusion zone size of $4\sqrt{t}$ (small weld population), all the DP800 welds failed in interfacial fracture mode. Even though the average fusion zone size for the small population is only ~10% smaller than the nominal fusion zone size (5.3 vs. 5.9 mm), both of its peak load and energy- absorption levels are significantly lower than those of the nominal welds, also with large degrees of scatter. However, further increase in fusion zone size from nominal (average 5.9 mm) to large (average 8.3 mm) only slightly enhances the peak-load and energy-absorption levels, particularly for the nominal welds that failed in nugget pullout mode. This can be attributed to the excessive indentation and significant metal loss due to expulsion for welds made at a higher current level.

TRIP800 Welds

Figure 14 illustrates the weld fusion zone size distribution and failure modes for the small, nominal, and large TRIP800 weld populations. It is shown that the weld fusion zone sizes were relatively well controlled for the TRIP800 small populations with all the samples failing in interfacial fracture mode. Since the small population has the target fusion zone size of $4\sqrt{t}$, the results in Figs. 14–16 show that interfacial fracture can be expected for TRIP800 welds with the conventionally recommended $4\sqrt{t}$ fusion zone size, and therefore, inconsistent weld performance with large scatters can be expected.

The average actual fusion zone size for the TRIP800 nominal population is around 7.7 mm, well above the predicted critical fusion zone size of 6.4. Because of this overwelding, 28 of the 30 TRIP800

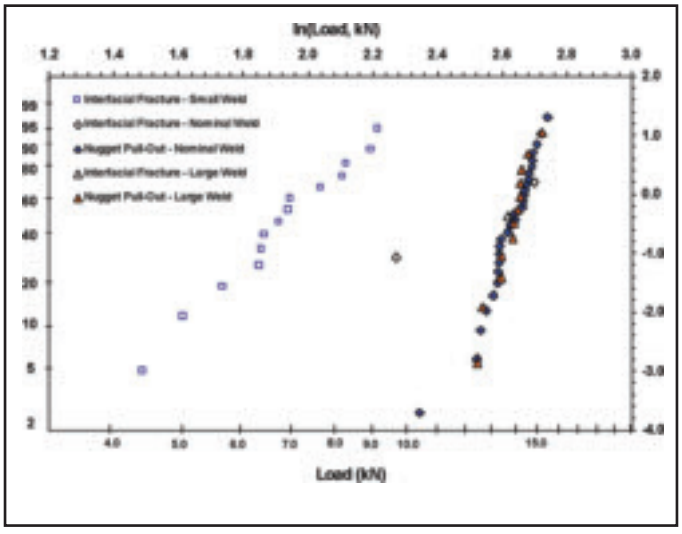

Fig. 15 — Peak load distributions for three weld populations in TRIP800.

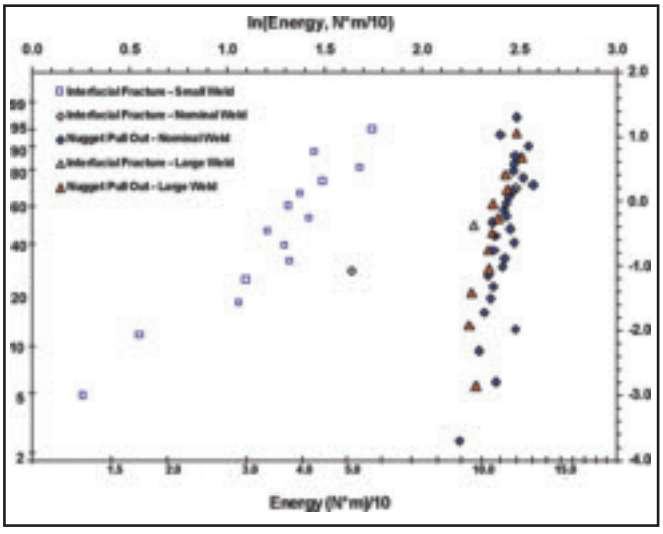

Fig. 16 — Distributions of energy absorption level for three weld populations in TRIP800.

nominal samples failed in nugget pull out and only two failed in interfacial fracture. The two samples that failed in interfacial fracture mode had fusion zone sizes of 6.2 mm and 6.8 mm. The average fusion zone size for the TRIP800 large weld population was 9 mm, and 14 of the 15 tested samples failed in nugget pullout mode. One sample with a considerably small fusion size in this population failed in interfacial fracture. Detailed examination of this weld also indicated some level of weld porosity at the periphery of the fusion zone.

Figures 15 and 16 show the effects of fusion zone size and weld failure mode on the peak load and total energy absorption of the RSW samples. The large slopes in Figs. 15 and 16 for the TRIP800 small population indicate large scatters in peak load and energy absorption for the welds failed in interfacial fracture. On the other hand, the much tighter slopes for the pullout welds in TRIP800 nominal and large populations indicate that welds failed in nugget pullout have a well-controlled peak load and energy absorption distributions with less performance variations. It is also interesting to note that even though the smallest weld in the TRIP800 large population failed in interfacial fracture mode, its peak load and energy absorption levels are comparable with the welds failed in pullout mode. In addition, the two interfacial fracture welds in the TRIP800 nominal population also indicate a large scatter in peak load and energy absorption. Note also that the peak load and energy absorption levels for the TRIP800 nominal and large populations are about the same. This can again be contributed to the significant weld indentation and expulsions for the TRIP800 large population.

It should be mentioned that the critical fusion zone sizes predicted here are for perfect welds without any porosity or cracks in the fusion zone. If porosity or voids exist at the periphery of the weld fusion zone, they could potentially change the local stress field around the weld tip and promote interfacial fracture for a particular weld. If severe weld porosity exists on the weld centerline, it could also potentially change the crack paths from interfacial fracture to partial interfacial fracture. It should also be noted that the critical fusion zone developed here is for cross-tension loading condition only. Under other loading conditions, such as lapshear or coach peel, the local stress fields around the welds are different. This study also suggests that different types of AHSS require different critical fusion zone sizes to ensure nugget pullout failure mode, even for the materials with the same strength grade, i.e., DP800 vs. TRIP800. Therefore, the practical challenge for ensuring AHSS weld quality lies in establishing an appropriate set of material-specific weld acceptance criteria that are easy to derive and implement in the automotive production environment.

Conclusions

Through experimental investigation, data analyses using statistical tools, and analytical study, the following conclusions can be derived from this research:

- The conventional weld size guidance of $4\sqrt{t}$ is not sufficient to produce nugget pullout failure mode for both DP800 and TRIP800 resistance spot welds.
- Analytical limit-load-based model together with microhardness measurements can be used to predict the critical fusion zone sizes for DP800. The predicted critical fusion zone sizes can serve as a lower bound limit to ensure nugget pullout failure mode such that desired level of weld performance can be achieved. For TRIP800, since the nominal weld size is much larger than the predicted critical size, additional study is needed to validate the accuracy of the prediction.
- At the critical fusion zone level, both interfacial fracture and nugget pullout were observed for the DP800 welds. Even though both failure modes offer similar distributions in terms of peak load, nugget pullout provides much higher energy absorption level than the interfacial fracture mode. This observation is different from previously reported aluminum RSW performance data, and it is due to the differences in microhardness characteristics between the aluminum and AHSS welds.
- Below the critical fusion zone sizes, interfacial fracture is the dominant failure mode with large load scatter and poor energy absorption.
- Above the critical fusion zone size, nugget pullout is the dominant failure mode with tightly controlled peak load and energy absorption distributions. Further increasing the fusion zone size beyond the critical size did not bring about linearly increased weld performance in terms of peak load and energy absorption.

Acknowledgments

Pacific Northwest National Laboratory is operated by Battelle for the U.S. Department of Energy under contract DE-AC06-76RL01830. The Department of Energy office of FreedomCar and Vehicle Technology funded this work. The DOE program manager is Joseph Carpenter.

References

1. Rathbun, R. W., Matlock, D. K., and Speer, J. G. 2003. Fatigue behavior of spot welded high-strength sheet steels. *Welding Journal* 82(8): 207-s to 218-s.

2. Matlock, D. K., Krauss, G., and Ziaebrahimi, F. 1984. Strain hardening of dual phase steels: an evaluation of the importance of processing history. *Deformation, Processing, and Structure*, ed. G. Krauss, pp. 47–87, ASM International, Materials Park, Ohio.

3. Riesner, M., Sun, X., Wu, S., Hwang, H.Y., and Low, E. 2000. Modeling and optimization of structural joints in automotive applications. *Proceedings of the International Crashworthiness Conference*, London, paper No. 2096.

4. Sun, X., and Dong, P. 2000. Analysis of aluminum resistance spot welding processes using coupled finite element procedures. *Welding Journal* 79(8): 215-s to 221-s.

5. Sun, X., Dong, P., and Kimchi, M. 1997. The coupled electrical-thermal-mechanical process associated with aluminum RSW. *Proceedings of the Seventh International Conference on Computer Technology in Welding*, ed. T. Siewert, pp. 447–457.

6. Sun, X., Stephens, E. V., Davies, R. W., Khaleel, M. A., and Spinella, D. J. 2004. Effects of fusion zone size on failure modes and static strength of aluminum resistance spot welds. *Welding Journal* 83(11): 188-s to 195-s.

7. Weld Quality Test Method Manual. 1997. Standardized Welding Test Method Task Force, Auto/Steel Partnership.

8. Sun, X., Stephens, E. V., Davies, R. W., Khaleel, M. A., and Spinella, D. J. 2004. Effects of failure modes on strength of aluminum resistance spot welds, SAE paper No. 2005-01-0906.

9. Girvin, B., Peterson, W., and Gould, J. 2004. *Development of Appropriate Spot Welding Practice for Advanced High-Strength Steels*, American Iron and Steel Institute, Pittsburgh, Pa.

10. Biro, E., and Lee, A. 2005. HAZ properties of various DP600 chemistries. *Canadian Welding Association Journal*, Spring, pp. 17–21.

11. Lin, S.-H., Pan, J., Wu, S.-R., Tyan, T. ,and Wung, P. 2002. Failure loads of spot welds under combined opening and shear static loading conditions. *International Journal of Solids and Structures* 39: 19–39.

12. Sun, X., and Khaleel, M. A. 2005. Performance optimization of self-piercing rivets through analytical rivet strength estimation. *Journal of Manufacturing Processes* 7(1): 83–93.

13. Sun, X., and Khaleel, M. A. 2005. Strength estimation of self-piercing rivets using lower bound limit load analysis. *Science and Technology of Welding and Joining* 10(5): 624–635.

14. *Metals Handbook*, Ninth Edition, Vol. 1. 1978. Properties and selection: irons and steels. ASM International, Materials Park, Ohio.

15. Ang, A. H.-S., and Tang, W. H. *Probability Concepts in Engineering Planning and Design*, Vol. 1, Basic Principles. John Wiley & Sons, New York, N.Y.

WELDING JOURNAL

Instructions and Suggestions for Preparation of Articles

Text

- approximately 1500–3500 words in length
- submit hard copy
- submissions via disk or electronic transmission — preferred format is Mac but common PC files are also acceptable
- acceptable disks include floppy, zip, and CD.

Format

- include a title
- include a subtitle or "blurb" highlighting major point or idea
- include all author names, titles, affiliations, geographic locations
- separate paper into sections with headings

Photos/Illustrations/Figures

- glossy prints, slides, or transparencies are acceptable
- black and white and color photos must be scanned at a minimum of 300 dpi
- line art should be scanned at 1000 dpi
- photos must include a description of action/object/person and relevance for use as a caption
- prints must be a minimum size of 4 in. x 6 in., making certain the photo is sharp
- do not embed the figures or photos in the text
- acceptable electronic format for photos and figures are EPS, JPEG, and TIFF. TIFF format is preferred.

Other

- illustrations should accompany article
- drawings, tables, and graphs should be legible for reproduction and labeled with captions
- references/bibliography should be included at the end of the article

Editorial Deadline

- January issue deadline is November 11
- February issue deadline is December 10
- March issue deadline is January 13
- April issue deadline is February 10
- May issue deadline is March 10
- June issue deadline is April 9
- July issue deadline is May 12
- August issue deadline is June 13
- September issue deadline is July 11
- October issue deadline is August 11
- November issue deadline is September 12
- December issue deadline is October 10

Suggested topics for articles

- case studies, specific projects
- new procedures, "how to"
- applied technology

Mail to:

Andrew Cullison
Editor, Welding Journal
550 NW LeJeune Road
Miami, FL 33126
(305) 443-9353, x 249; FAX (305) 443-7404
cullison@aws.org